Proceedings of ASME Turbo Expo 2022
Turbomachinery Technical Conference and Exposition
GT2022
June 13-17, 2022, Rotterdam, The Netherlands

GT2022-81345

ASSESSMENT OF A CONJUGATE HEAT TRANSFER METHOD ON AN EFFUSION COOLED COMBUSTOR OPERATED WITH A SWIRL STABILIZED PARTIALLY PREMIXED FLAME

A. Amerini*, S. Paccati, L. Mazzei & A. Andreini
Department of Industrial Engineering
Heat Transfer and Combustion group
University of Florence
Florence, Italy
*alberto.amerini@unifi.it

ABSTRACT

Computational fluid dynamics play a crucial role in the design of cooling systems in gas turbine combustors due to the difficulties and costs related to experimental measurements performed in pressurized reactive environments. Despite the massive advances in computational resources in the last years, reactive unsteady and multi-scale simulations of combustor real operating conditions are still computationally expensive.

Modern combustors often employ cooling schemes based on effusion technique, which provides uniform protection of the liner from hot gases, combining the heat removal by means of heat sink effect with liner coverage and protection by film cooling. However, a large number of effusion holes results in a relevant increase of computational resources required to perform a CFD simulation capable of correctly predicting the thermal load on the metal walls within the combustor. Moreover, a multi-physics and multi-scale approach is mandatory to properly consider the different characteristic scales of the several heat transfer modes within combustion chambers to achieve a reliable prediction of aero-thermal fields within the combustor and wall heat fluxes and temperatures. From this point of view, loosely-coupled approaches permit a strong reduction of the calculation time, since each physics is solved through a dedicated solver optimized according to the considered heat transfer mechanism. The object of this work is to highlight the capabilities of a loosely-coupled unsteady multi-physics tool (U-THERM3D) developed at the University of Florence within ANSYS Fluent.

The coupling strategy will be employed for the numerical analysis of the TECFLAM effusion cooled swirl burner, an academic test rig well representative of the working conditions of a partially premixed combustion chamber equipped with an effusion cooling system, developed by the collaboration of the Universities of Darmstadt, Heidelberg, Karlsruhe, and the DLR. The highly detailed numerical results obtained from the unsteady multi-physics and multi-scale simulation will be compared with experimental data to validate the numerical procedure.

NOMENCLATURE

c	Progress variable	[-]
d	Effusion holes diameter	[mm]
D	Pilot duct diameter	[mm]
f	Shielding function	[-]
m	Mass flow	[g/s]
P	Pressure	[MPa]
T	Temperature	[K]
x	Streamwise direction	[mm]
Y	Species mass fraction	[-]
y	Spanwise direction	[mm]
Z	Mixture fraction	[-]

Acronyms

SBES	Stress-Blended Eddy Simulation
CARS	Coherent Anti-Stokes Raman Spectroscopy
CFD	Computational Fluid Dynamics
CFL	Courant-Friedrichs-Lewy
CHT	Conjugate Heat Transfer
DES	Detached Eddy Simulation
FGM	Flamelet Generated Manifold
LES	Large Eddy Simulation
OH-PLIF	Planar Laser-Induced Fluorescence of OH
PDF	Probability Density Function
PIV	Particle Image Velocimetry
RANS	Reynolds Averaged Navier Stokes
SST	Shear Stress Transport
TIT	Turbine Inlet Temperature
TPT	Thermographic Phosphor Thermometry

Greek

α	Effusion hole angle	[°]
τ	Sub-grid stress tensor	[Pa]
ψ	Generic variable	[-]

ω	Turbulence frequency	[s^{-1}]

Subscripts

eff	Effusion cooling air
eq	Equilibrium
f	Fuel
ox	Oxidizer air

1. INTRODUCTION

Progressive increases in gas turbine performances through higher Turbine Inlet Temperature and operating pressures have led to ever-increasing thermal loads on the metal components of the aero-engines. Therefore, accurate estimation of the metal liners temperature within combustion chambers is fundamental to achieve an effective design of cooling systems and therefore the safe operability of the whole engine. Experimental tests under real engine operating conditions are extremely complex and expensive due to all the difficulties associated with the high temperatures that develop in the combustion chamber. This is why a large part of the design phase of the cooling systems is carried out with numerical approaches. From this point of view, Computational Fluid Dynamics (CFD) simulation of Conjugate Heat Transfer (CHT) problems are extremely useful for the study of fluid-solid heat transfer phenomena which occur inside the engines but at the same time, it is very complex to properly model them. The first critical issue is the modeling of the cooling system. The most used for combustion chambers is based on multi-perforated liners [1], which guarantee excellent performance thanks to the removal of heat through the heat sink effect, related to the passage of coolant inside the holes, combined with protective film layer that forms at the outlet holes between the hot gases and the metal wall [2], [3]. This cooling system is suitable for the new combustor architectures according to the new emission standards, set in Flightpath 2050 [4], [5], where a reduced amount of air is used for cooling to have lean combustion by means of a strict control of the equivalence ratio in the primary zone [6]. However, accurate numerical modeling of the effusion holes requires a high computational cost, especially when there is an interaction with a swirling flow [7]–[10].

The other critical aspect is related to the strong unsteadiness which is typical of the reactive flow within aeroengine combustors, highly affecting the intensity of the thermal loads on the metal liners. Low-cost numerical computational methods such a Reynolds-Averaged Navier–Stokes (RANS) simulation can be exploited in the preliminary stages of the combustor design but do not allow accurate solution for heat transfer problems, which are dominated by the turbulent interaction between aerothermal field, combustion, and heat removal due to cooling systems. Approaches based on Large Eddy Simulation (LES), or at least, Detached Eddy Simulation (DES) approaches [11], are needed for these types of problems [12]. In particular, the second-mentioned methodology, being a hybrid RANS/LES approach [13], allows having accurate results with moderate computational costs, combining the strengths of the two approaches. Although this numerical strategy is more efficient, a fully coupled CHT calculation would lead to an unmanageable computational cost due to the non-negligible difference between the characteristic times scales of the different heat transfer mechanisms and between convective and conductive phenomena. Loosely coupled approaches [14], [15] reduce computational costs because each heat transfer mechanism is solved in a dedicated simulation, which specific quantities being exchanged between them.

The present work focuses on the numerical study of a gas turbine combustor model with the accurate multi-physics multi-scale tool U-THERM3D, developed within the ANSYS Fluent suite by the authors [16], [17]. The objective of the work is to perform the first simulation of the TECFLAM swirl burner, equipped with an effusion cooled metallic liner, in order to obtain an accurate prediction of the wall temperature distribution.

The first part of the paper will describe the experimental test case, then the U-THERM3D approach will be described together with the employed numerical setup. Finally, the obtained results will be shown and discussed, comparing them with the available experimental data.

2. EXPERIMENTAL TEST CASE

In the present work an unsteady, multi-scale and multi-physics simulation is carried out on a single sector effusion cooled swirler burner developed and tested by the cooperation between the universities of Darmstadt, Heidelberg, Karlsruhe, and the DLR, named as TECFLAM combustor. The main objective of the experimental investigations was a detailed quantitative characterization of the confined swirling diffusion flames stabilized on the gas turbine combustor model under close-to-reality operating conditions and fueled with natural gas.

In Figure 1 two views of the single sector combustor are reported. The main fuel injection is via radial ducts, the fuel then mixes with the oxidizing air and passes through the movable block swirler. This type of swirler has already been numerically studied by Nassini et al. [18] in its unconfined version. The rig has also a central pilot duct with a diameter of 2.5mm for fuel supply so that it can operate with a fully premixed or partially premixed flame. The flametube has a square cross-section and features three quartz optical access windows. The underneath liner has effusion cooling with 145 circular holes, with a diameter of 2mm and an angle of 30 degrees to the direction of flow. The cooling system has a dedicated supply system in which air is forced through the perforated plate. A sketch of the effusion cooling pattern geometry is shown in Figure 2.

The combustor was tested under several operating points and detailed measurements were carried out with different techniques. The flow field was measured under both reactive and non-reactive conditions using Particle Image Velocimetry (PIV) in [19] whereas, the temperature profiles were obtained using the Coherent Anti-Stokes Raman Spectroscopy (CARS) technique. Greifenstein et al. [20] performed a flame structure study is performed with the Planar Laser-Induced Fluorescence of OH (OH-PLIF) to investigate the flame-cooling air interaction.

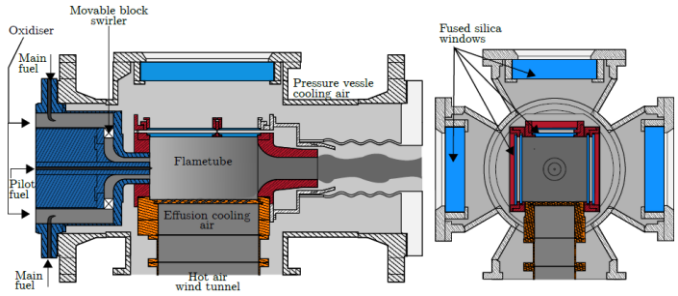

FIGURE 1: CROSS AND LONGITUDINAL SECTION OF TECFLAM BURNER ADAPTED FROM [19], [20]

In the above-mentioned work, the thermal maps on a portion of the effusion cooled liner are obtained by 2D Thermographic Phosphor Thermometry (TPT). For further details on measurement techniques and the experimental apparatus, please refer to the above-mentioned works.

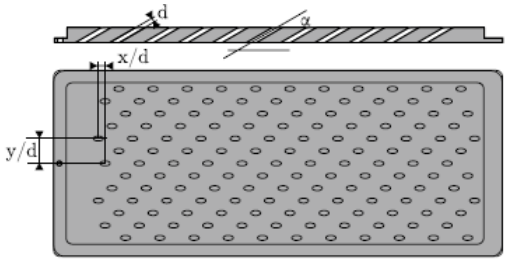

FIGURE 2: EFFUSION COOLING PATTERN, FROM [20]

Only one operating condition of those analyzed by Greifenstein et al. in [20] has been investigated in this current work, and the corresponding operating conditions are shown in Table 1.

TABLE 1: INVESTIGATED OPERATING CONDITIONS

Name	*Symbol*	*Value*	*Unit*
Oxidizer mass flow	$\dot{m}_{ox}$	30	g/s
Oxidizer temperature	T_{ox}	623	K
Eff. cooling mass flow	$\dot{m}_{eff}$	7.5	g/s
Eff. Cooling temperature	T_{eff}	623	K
Total fuel mass flow	$\dot{m}_f$	1.128	g/s
Operating pressure	P	0.25	MPa
Swirl number	S	0.7	-
Staging ratio	SR	10	%

In this study only the partially premixed flame is analyzed where the combustor works with a pilot fuel percentage of 10% of the total, indicating this quantity with the name "staging ratio" in the previous table.

3. NUMERICAL METHODOLOGY

All numerical analyses were carried out with the 2019R1 version of the commercial CFD solver ANSYS Fluent [21]. In the following sections, the employed numerical models will be described.

3.1 Turbulence Modelling

The hybrid RANS/LES approach named Stress-Blended Eddy Simulation (SBES) [21], [22] was used to carry out most of the simulations. This model belongs to the family of DES methods in which wall stresses are solved using a RANS approach whereas, regions subjected to massive separations and unguided flows are solved using a LES approach. This numerical method allows optimal handling of turbulence models as a function of the local flow field, improving the quality of the solution that would be provided by a fully RANS simulation but at the same time reducing the computational efforts for boundary layer modeling that would be mandatory with a pure LES simulation. The switch between RANS and LES behaviors is uniquely controlled by means of a blending (or also called "shielding") function f_{SBES}, which is defined as follows:

$$\tau_{ij}^{SBES} = f_{SBES} \cdot \tau_{ij}^{RANS} + (1 - f_{SBES}) \cdot \tau_{ij}^{LES} \quad (1)$$

where, τ_{ij}^{SBES} and τ_{ij}^{RANS} are, respectively, the LES and RANS parts of the sub-grid stress tensor. In this work, the RANS sub-grid stress is modeled with the k-ω SST model [23], while the LES part is calculated with the Dynamic-Smagorinsky model [24].

3.2 Combustion Modelling

The Flamelet Generated Manifold (FGM) combustion model has been considered to describe the reactive behavior of the flame. A two-dimensional manifold is obtained by solving the set of laminar adiabatic 1-D flamelets (opposed jets). With this model, the chemical state and the reactive process depend only on the mixture fraction Z and the progress variable c [25], defined as a mass fraction ratio of CO and CO_2 as follow.

$$c = \frac{(Y_{CO} + Y_{CO2})}{(Y_{CO} + Y_{CO2})_{eq}} \quad (2)$$

The manifold $\phi(Z, c)$ was generated with 64x64 points using the ANSYS Fluent built-in tool in which the turbulent interaction is included by assuming a priori a β-Probability Density Function (β-*PDF*) for the two control variables [26]. The integrated value of a generic turbulent variable $\psi(Z, c)$, assuming Z and c to be statistically independent of each other, results in:

$$\tilde{\psi} = \iint \psi(c, Z) PDF(\tilde{c}, \tilde{c}''^2) PDF\left(\tilde{Z}, \tilde{Z}''^2\right) dZdc \quad (3)$$

where $\tilde{c}, \tilde{Z}$ are the mean values and $\tilde{c}''^2, \tilde{Z}''^2$ the variances values of mixture fraction and progress variable that are obtained by the resolution of two additional transport equations. The turbulent-chemistry interaction is modeled using the finite rate closure for the $\tilde{c}$-source term [21]. The same natural gas mixture as used in the experimental reference work conducted by Greifenstein et al. [20] was used for the simulations, adopting the GRImech 3.0 [27] reaction mechanism with 325 reactions and 53 species.

3.3 U-THERM3D

The U-THERM3D numerical strategy was developed in the ANSYS Fluent suite and designed to optimize the resolution of CHT unsteady problems by desynchronization of the time-steps employed to solve all the involved heat transfer phenomena. Generally, the goal is to model the three main heat transfer modes, convection, (intrinsically dependent on flow turbulence and chemical reaction), conduction, and radiation. In the U-THERM3D approach, each of these modes is solved in a dedicated simulation, running with a parallel coupling strategy. This strategy allows the use of the most suitable numerical setup and calculation grid for each simulation involved.

The U-THERM3D tool and its steady state version (THERM3D) [28]–[30] have been extensively validated on several test cases. The full capabilities of the U-THERM3D tool, are described in the work of Bertini et al. [16] in which not only the radiative heat transfer is considered but also the effusion cooling system is solved with a simplified 0D approach, based on [31], to significantly reduce the computational cost of the simulation. In [17] U-THERM3D is adopted to obtain an accurate prediction of the wall temperature distribution for a combustor with a non-premixed sooting flame.

In this work, a simplified version of the described approach will be used, since the contribution of radiative heat transfer will be neglected due to the typical small luminosity of methane flames. Therefore, only the interaction between the fluid and the solid domains will be modeled. A representation of the procedure workflow is shown in Figure 3.

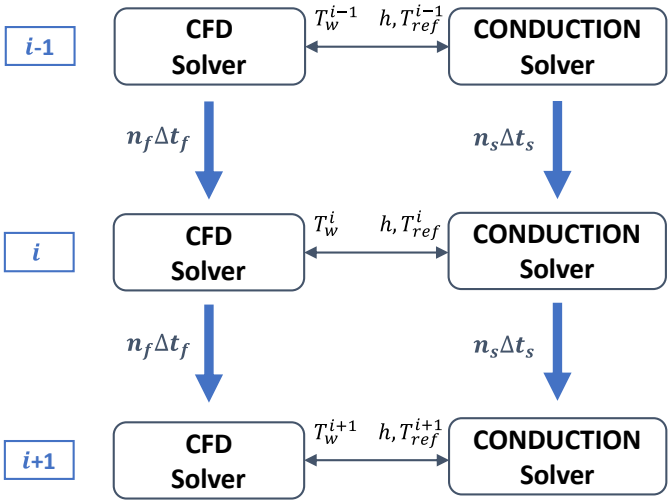

FIGURE 3: U-THERM3D SIMPLIFIED PROCEDURE

CFD and conduction solvers advance in time with their own and proper time-step, while data on the coupled surfaces of the two simulations are exchanged regularly with a user-defined frequency to update the boundary conditions. In this work, the coupling between the two simulations occurs every 10 fluid and 30 solid time steps. For numerical stability reasons, the heat flux of the CFD simulation is firstly converted in an equivalent Robin boundary condition and then transferred to the solid simulation.

3.4 Setup

As mentioned in the previous section, the U-THERM3D approach requires the setup of two different simulations to solve convective and conductive heat transfer problems. For the SBES CFD simulation, the pressure-based algorithm SIMPLEC was used, all equations were solved with a second-order upwind scheme and a second order implicit formulation for time discretization were employed. Regarding the fluid time step, it has been set to $1e^{-6}$s to ensure a Courant-Friedrichs-Lewy (CFL) condition almost equal to 1 over the entire calculation domain. The CFD domain is shown in Figure 4 (solid plate and effusion plenum are deliberately shifted to highlight the coupled walls). Regarding the coupled boundary conditions, in addition to the two faces of the plate shown in Figure 4, the lateral surfaces of the cylindrical effusion holes were also coupled. For each inlet, the corresponding mass flow rate value and temperature indicated in Table 1 was set, while for the outlet the operating pressure is imposed. The temperature of the pilot jet was set at 333K, following what was declared by Greifenstein et al. in the reference works [19], [20].

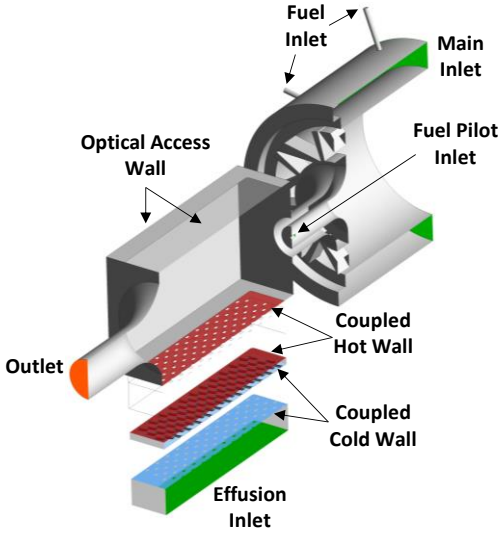

FIGURE 4: COMPUTATIONAL DOMAIN

Concerning the duct pilot fuel modeling, the length of the pipe has been reduced with respect to the original dimension after a first SBES simulation carried out on the complete domain. This first simulation showed a RANS-like solution within the pilot duct and next to the tube outlet due to a SBES shielding function equal to 1, resulting in an underestimation of turbulence and mixing levels in these regions. To improve the quality of the simulation in these areas it was decided to reduce the pilot duct extension according to the geometry reported in Figure 4 and to model the inlet with a fully developed velocity profile defined by means of the power law [32] and a mean value of 12.73 m/s to match the experimental fuel mass flow rate. To ensure a level of turbulence required for a LES-like solution, a synthetic turbulence generation [21] at the fuel pilot inlet was also imposed. The properties of the reactive mixture were imposed

temperature dependent and derived from dedicated calculations carried out in Cantera [33]. As discussed above, radiative heat transfer was neglected in this first study of the TECFAM burner, due of an assumed insignificant emissivity of the gaseous methane-air flame. On quartz surfaces, it was decided to impose a fixed temperature for the three optical accesses with which the flametube is equipped. Since in Greifenstein et al. work [19], [20] there is no information about the thermal characterization of quartz windows, a numerical campaign based on directly coupled CHT RANS simulations was carried out in order to study the effect quartz walls temperature on the behavior of the simulated combustor. Three simulations were carried out: the first one with adiabatic quartz walls whereas the other two imposing a uniform temperature of 1300K and 1500K respectively. The results obtained were compared with the experimental temperature profile on the combustor centerline in Figure 5.

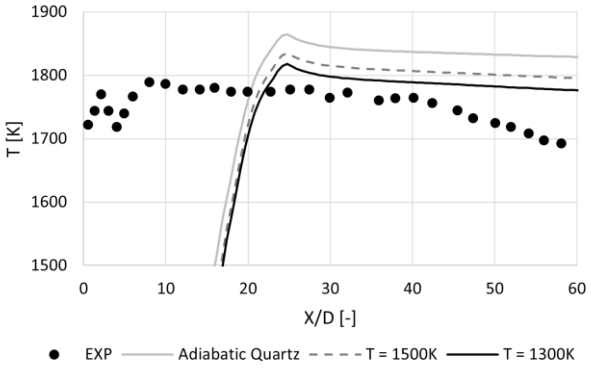

FIGURE 5: SENSITIVITY ANALISYS RESULTS IN TERM OF TEMPERATURE DISTRIBUTIONS ALONG THE COMBUSTOR CENTERLINE

For the subsequent unsteady simulations, the actual objective of the work, a uniform temperature of 1300K on the three optical accesses was chosen as the reference condition for the quartz as it is the condition that approximates most closely the experimental result. This value is also comparable to the typical operating temperatures of the quartz employed for this type of laboratory application.

Concerning the solid domain simulation, only the energy equation is solved as only heat transfer by conduction is present. Due to the temporal desynchronization of the loosely coupled approach, the solid domain simulation could adopt a time step of $1e^{-3}$s consistent with the characteristic timescales of the conductive phenomenon. The solid was modeled as an alloy metal with polynomial temperature-dependent properties.

Both computational grids were generated in ANSYS Meshing. A mesh of 146M tetrahedral elements with 5 prismatic layers in the near-wall region was generated for the CFD simulation and converted to 42M polyhedral elements, as shown in Figure 6. Several local refinements have been introduced to ensure correct resolution of turbulent structures. Compared to the nominal mesh sizing of 1mm, the swirler and primary zone have been discretized with elements of 0.45mm. For the pilot jet duct and the area immediately downstream, an additional thickening has been inserted, using in this area a size of 0.1mm. An element size of 0.15mm was employed for the discretization of the effusion holes, whereas in the area near the hot wall a sizing of 0.75mm was adopted.

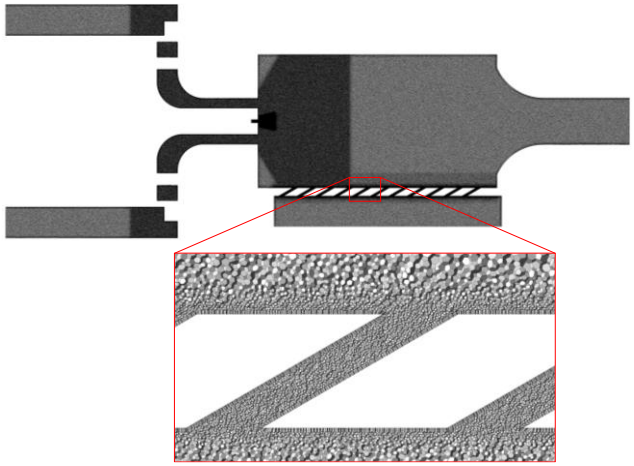

FIGURE 6: CFD MESH GRID

Mesh sizing was defined according to [34] which suggests to adopt a grid resolution based on the local values of turbulence Reynolds number and of Kolmogorov length scale for a proper scale resolving simulation.

The calculation grid defined in this way allows the resolution of the 80% of the turbulent kinetic energy, thus satisfying the Pope criterion [35] which gives an indication of the good quality of the obtained LES solution. The above criterion is widely used in applications involving reactive flows within combustion chambers [36], [37] and it is often reported in terms of M, the ratio of modelled to resolved turbulent kinetic energy as shown in Figure 7. As can be seen, the resolved turbulent kinetic energy is well above the 80% threshold, resulting in M values less than 0.2 over a large part of the calculation domain.

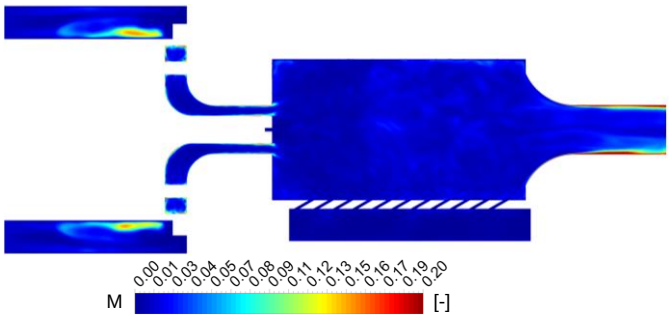

FIGURE 7: POPE CRITERION

Regarding the conductive simulation, a mesh grid with a uniform tetrahedral element size of 0.75mm has been generated with a total number of elements equal to 7M.

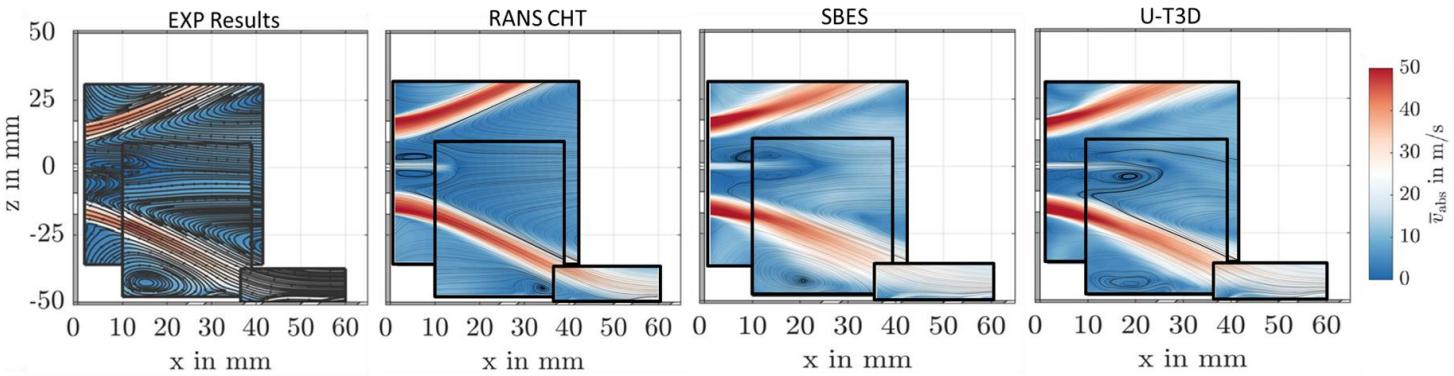

FIGURE 8: REACTIVE FLOW FIELD COMPARISON OF THE COMBUSTOR PRIMARY ZONE BETWEEN EXPERIMENTAL RESULTS FROM [19] AND DIFFERENT NUMERICAL APPROACHES ADOPTED

4. RESULTS

This section presents and discusses the results obtained from the simplified U-THERM3D procedure. The achieved multi-physics results will be compared with the experimental results and with two simulations, a steady state RANS CHT and a SBES fluid simulation with adiabatic walls. Firstly, the results of the velocity field within the combustor will be discussed both qualitatively and quantitatively by employing profiles of velocity components along the radial direction. Subsequently, the temperature maps will be presented and finally, the effusion system will be studied by analyzing the wall temperature maps.

Before examining the results, a brief cost-effectiveness offered by the loosely coupled U-THERM3D approach is reported. The calculation time for a strongly coupled SBES simulation is only estimated as this type of simulation would lead to an unfeasible computational cost. Setting the simulated physical time for the solid domain to 60s, the U-THERM3D simulation needs 345k cores per hour against 576M for the equivalent CHT simulation.

4.1 Velocity fields

The typical velocity structures of a swirling flow are well evident in all the contours shown in Figure 8. In the lower-left corner of the flametube the Outer Recirculation Zone (ORZ) vortex is well developed. As expected, the experimentally measured vortex structures are predicted quite accurately by the unsteady simulations compared to those obtained with the steady state approach. This can also be seen in the proximity of the pilot jet injection within the Inner Recirculation Zone (IRZ). Comparing the two unsteady simulations, it is possible to note some differences in the behavior near the effusion-cooled wall. This is because in the SBES simulation the adiabatic wall is considered, while in the U-THERM3D simulation the coupling with the solid plate provides greater temperature variations that affect the local velocity field. These considerations can also be confirmed by considering the one-dimensional radial profiles of the velocity components, reported in Figures 9 and 10. The graphs show the axial and radial velocity distributions at three different axial locations, indicated in dimensionless terms, of the combustor: a section close to the burner at X/D = 2, one in the primary zone near the first row of effusion cooling holes at X/D = 10 and the last one at the end of the combustor at X/D = 68. The comparison of tangential velocity components is only computed on the last two axial locations as not experimentally measured in the first section.

The numerical approaches predict a higher axial velocity for the pilot jet about twice to the experimental data, whereas for the other radial positions the agreement is within 10% of the experimental reference value. As will be described in the following section, the modeling of the fuel pilot jet will have a strong impact on the whole behavior of the flame as it will vary the local mixture fraction conditions, influencing therefore the local reactivity.

Observing the axial velocity profiles in Figure 10, the improvement introduced by unsteady numerical approaches in

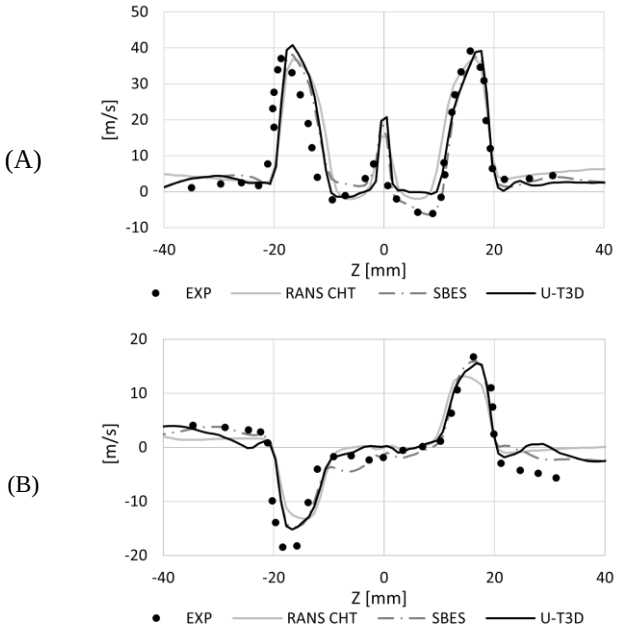

FIGURE 9: RADIAL DISTRIBUTIONS OF AXIAL (A) AND RADIAL (B) VELOCITY COMPONENTS AT X/D = 2

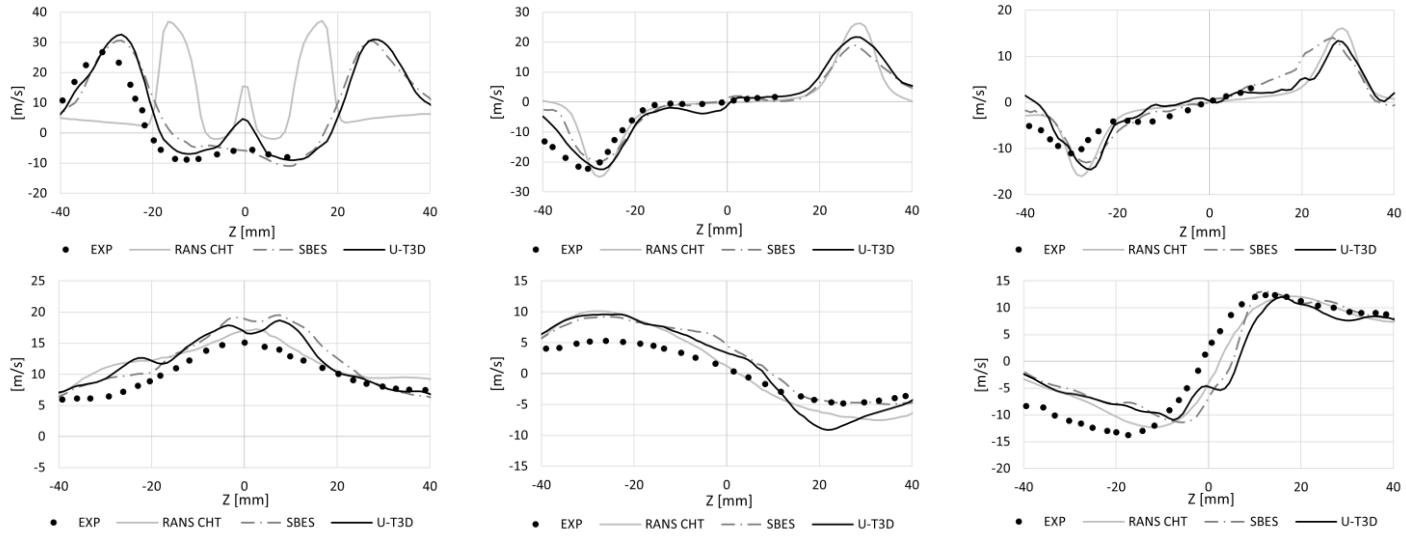

(A) (B) (C)

FIGURE 10: RADIAL DISTRIBUTIONS OF AXIAL (A), RADIAL (B) AND TANGENTIAL VELOCITY COMPONENTS AT X/D = 10 (TOP) AND X/D = 68 (BOTTOM)

terms of velocity field and swirling flow prediction is highlighted. At the same time multi-physics simulations predict excessive penetration of the pilot jet that is also evidenced in the axial velocity profiles at X/D = 10, confirming what has already been discussed about the profiles in Figure 9.

Concerning again the axial velocity profiles, there is a slight shift in terms of position of the bottom swirl jet interacting with the cooled wall. Near the flametube outlet, the numerical velocity profiles overestimate about 20% the experimental ones. In this zone, however, the experimental velocity profiles are subject to greater variability, as can be seen from the graphs in Figure 11 which show the comparisons between the radial profile of the root mean square (RMS) velocity components. Both unsteady simulations are reasonably in agreement with experimental RMS so turbulent fluctuations are correctly predicted by the SBES approach. In the primary zone, the main differences between experiment and numerical results are in proximity of the effusion plate, where the turbulent contribution of the interaction between main swirling flow and effusion jets is observed to be underestimated by the numerical approaches.

4.2 Temperature fields

Figure 12 shows the temperature maps of the flametube of the three different numerical approaches on the symmetry plane of the combustor; for the two unsteady simulations, the time-averaged maps are shown.

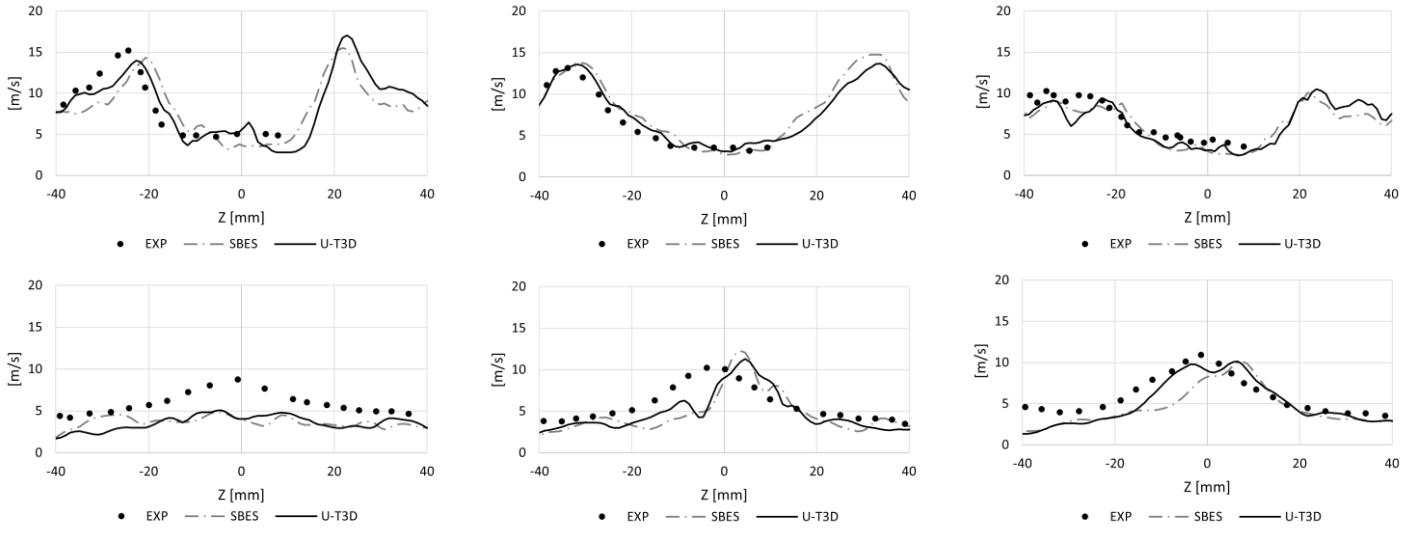

(A) (B) (C)

FIGURE 11: RADIAL DISTRIBUTIONS OF AXIAL (A), RADIAL (B) AND TANGENTIAL (C) RMSE VELOCITY COMPONENTS AT X/D = 10 (TOP) AND X/D = 68 (BOTTOM)

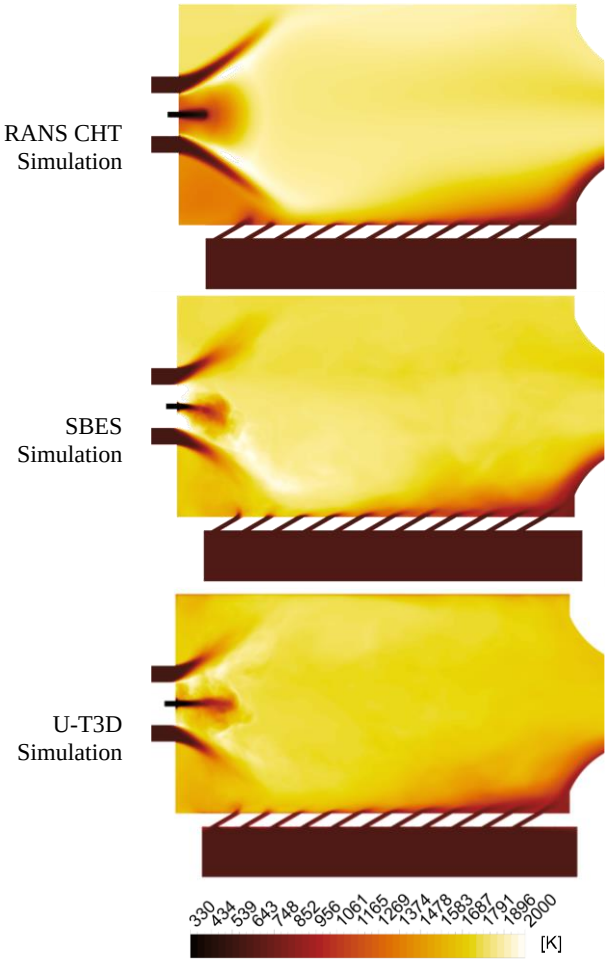

FIGURE 12: TEMPERATURE MAPS ON XZ MIDPLANE OF THE COMBUSTOR: (TOP) RANS CHT, (MIDDLE) SBES, AND (BOTTOM) U-THERM3D SIMULATIONS

The temperature maps obtained from the three simulations are consistent with each other. While for the multi-physics simulations (RANS CHT and U-THERM3D) a rather symmetrical flame structure is recognizable this is not the case for the SBES simulation where only the aerothermal field is resolved. Furthermore, it is possible to notice a reduction in temperature inside the combustion chamber due to an accurate resolution of turbulence and thus of mixing which increase heat transfer combined with increased diffusion of the fuel pilot jet.
For the U-THERM3D simulation, this aspect is even more evident, but it is important to remember that in this simulation the temperature of the quartz optical accesses has been imposed to consider the heat loss towards the outside calculation domain. This boundary condition combined with the heat removed by the effusion cooling system leads to strong cooling of the flame which then causes a lower temperature in the entire combustion chamber. The penetrating behavior of the pilot fuel jet can be observed for all simulations. For the SBES simulation, the strong IRZ near the bluff body, visible in Figure 8, leads to an increase

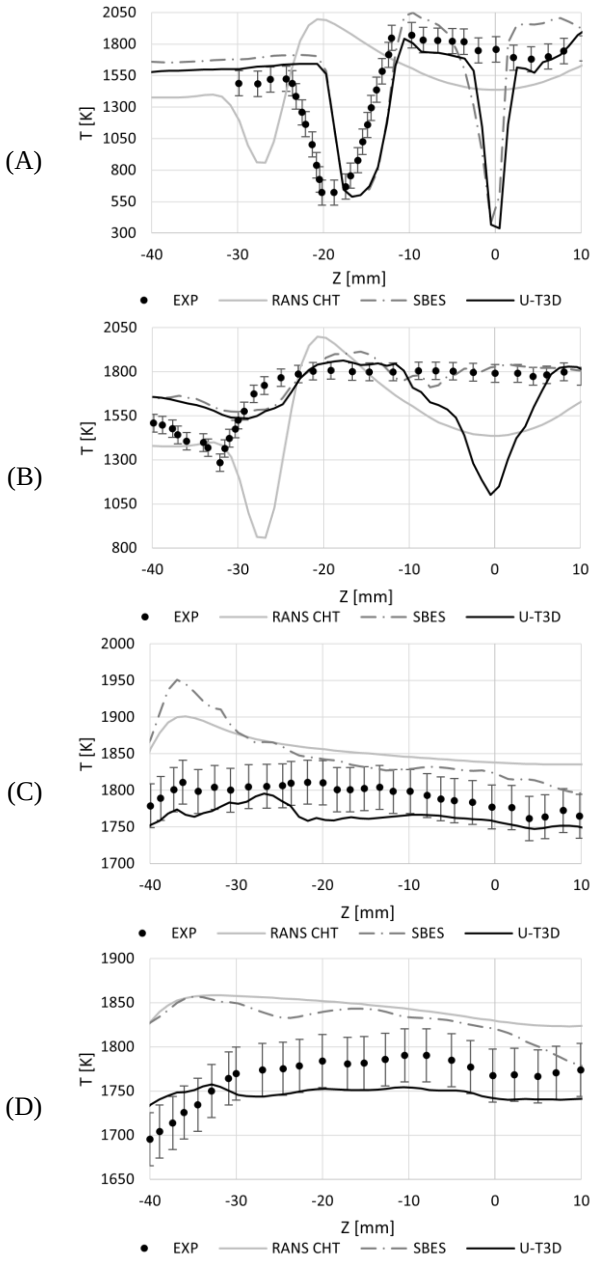

FIGURE 13: TEMPERATURE RADIAL DISTRIBUTIONS AT X/D = 2 (A), X/D = 10 (B), X/D = 20 (C) AND X/D = 30 (D)

in temperature, due to a higher predicted mixing between fuel and oxidant and so to a higher reaction rate.

This phenomenon is also present in the U-THERM3D simulation, but it is of lesser magnitude since the recirculation vortex at the sides of the pilot jet is weaker, whereas it is almost absent in the steady simulation due to the underestimation of turbulence typical of RANS approach.

For a deeper understanding from a quantitative point of view, radial temperature profiles are shown for different axial locations of the combustor in Figure 13. The black bars referring to the experimental profile indicate the uncertainty of the measurement itself. It is evident from the temperature profiles

that the numerical procedures are not fully in agreement with the experimental measurements near the pilot jet area but at the same time for the axial sections located downstream in the combustion chamber, the simulations tend to predict the same temperature as the experimental one.

Although the test rig under consideration is academic, it is affected by an extremely complex aerothermal field, and the conditions in the primary zone are highly dependent on the behavior of the pilot jet. In fact, the modeling of a partially premixed flame is particularly critical, moreover, the uncertainties linked to the thermal boundary conditions (not taking into account the pilot fuel heating that may occur during the passage through the swirler system) can have a significant impact on the reactivity of the mixture in the primary region.

To further highlight the criticality related to a proper fuel pilot modeling, temperature profiles on the combustor centerline are reported in Figure 14. In this case, the black bars relative to the experimental result indicate the minimum and maximum measured values. Regarding the numerical simulations, two different post-processes have been carried out: the continuous line represents the result similar to the experimental case on a single line, while the dashed lines were obtained by averaging the temperature on a circular sector of 2.5mm. This second procedure was implemented as a consequence of a detailed analysis of the experimental results. According to the CARS experimental measurements, a very high temperature was found to be that of unreacted fuel close to the bluff body. Averaging over a circular sector the non-zero beam diameter is considered.

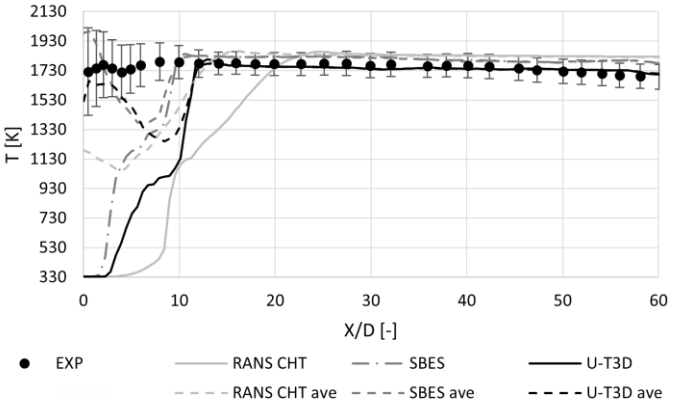

FIGURE 14: TEMPERATURE DISTRIBUTIONS ALONG THE COMBUSTOR CENTERLINE

Although with the second post-process the agreement with the experimental data tends to improve, the gap between the measured and predicted temperature in the pilot jet zone is still high. This is probably related to underpredicted turbulence mixing in the region next to the pilot inlet due to the imposed boundary conditions. This aspect could be improved by using profiles also for the turbulent quantities instead of the integral values currently used and derived from the fully developed velocity profile as previously described. After the mixing zone and the complete reaction of the pilot fuel (about 10 times the pilot duct diameter), the numerically predicted temperatures agree with the experimental values.

The differences between the two unsteady simulations can depend on the excessive heat removal by the quartz walls of the U-THERM3D simulation. Support of this thesis is seen in Figure 15, which shows the temperature maps of the XY midplane of the flame tube.

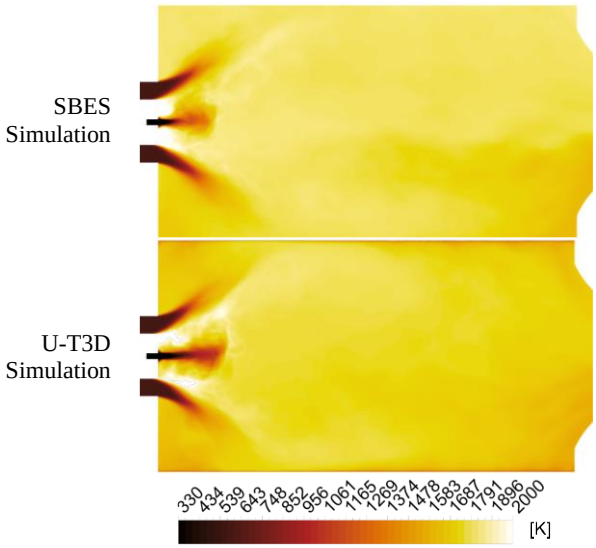

FIGURE 15: TEMPERATURE MAPS ON XY MIDPLANE OF THE COMBUSTOR: (TOP) SBES AND (BOTTOM) U-THERM3D SIMULATIONS

Focusing the attention on the primary zone it is possible to see the influence of the boundary condition imposed on the quartz walls of the U-THERM3D simulation compared to an adiabatic walls condition as imposed in the SBES simulation, leading to a good prediction for the loosely coupled simulation, while the simulation of the gaseous phase only leads to an inevitable overestimation of the temperatures along the combustor centerline.

Finally, the impact that the thermal boundary condition on the quartz walls has on the entire primary combustor zone is further emphasized by focusing on the ORZ. It is observed that the U-THERM3D simulation is significantly cooler than the same zone in the SBES simulation. This leads to excessive cooling of the flame with consequent change of the local reactivity of the flame and therefore flow characterization inside the IRZ.

4.3 Wall temperature and effusion cooling behavior

The wall temperature maps on the hot side of the effusion cooled plate obtained for the two multi-physics simulations are shown in Figure 16. The maps have an extension of 20 mm in spanwise direction centered symmetry plane of the effusion plate while having an axial development (flow direction from left to right) of 50 mm and start close to the first central row of effusion holes.

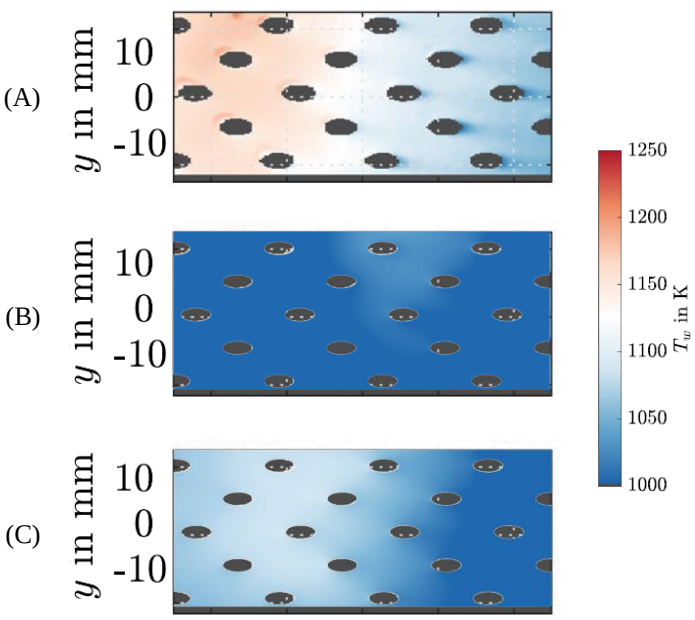

FIGURE 16: WALL TEMPERATURE MAPS: EXPERIMENTAL RESULTS ADAPTED FROM [20] (A), RANS CHT SIMULATION (B), AND U-THERM3D SIMULATION (C)

The numerical distributions underestimate the values obtained experimentally. Whereas the RANS CHT simulation fails to predict experimental data, the U-THERM3D approach allows partial agreement with reference results. The wall temperature map achieved with the unsteady simulation is similar, at least in shape, to the experimental one and correctly predicts the thermal gradient in the axial direction.

A quantitative comparison of the wall temperature profiles is shown in Figure 17. Also, in this case, the black bar relative to the experimental data indicates the measured uncertainty. For each case two curves are reported, the continuous lines represent the wall temperature along the liner centerline intercepting four effusion holes rows: these parts are masked. The dotted lines, on the other hand, represent the wall temperature between one row and the next in the spanwise direction without intercepting any holes. As previously said, the simulations tend to underpredict the wall temperatures. Although the underestimation is on the order of 100K, the U-THERM3D simulation is able to qualitatively predict the experimental temperature trend, showing a great improvement with respect to the steady simulation in the first region. The better predicted flame-wall interaction and turbulence lead to a more reliable computation of the local heat fluxes. The fact that both numerical simulations predict the same wall temperature after an axial location of X/D = 25 partially agrees with what has been reported in [20]. In fact, several parameters, including the swirl number and flame type, are varied parametrically in the experimental work, and the author concludes that after X/D = 30 the wall temperature only depends on the injected coolant flow rate.

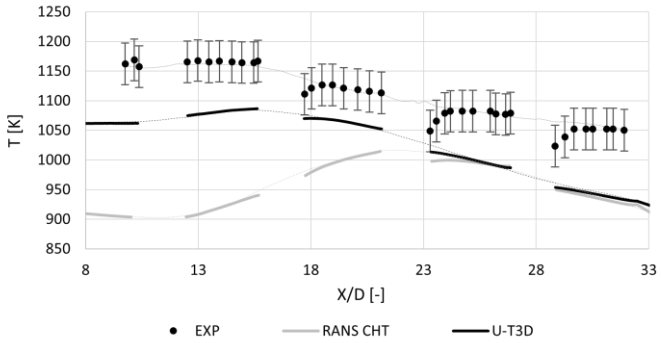

FIGURE 17: WALL TEMPERATURE PROFILES (LONG DASHED LINES) ALONG CENTERLINE AND (DOTTED LINES) ALONG LINES BETWEEN ROWS

The fact that this distance is reduced in the numerical approach may be due to an underestimation of the interaction between the main and coolant flow. To highlight these aspects, the velocity magnitude and radial component velocity contours at the exit of the centerline of the second and third rows of effusion holes are shown in Figure 18. As it can be seen from the velocity fields, the radial component of the swirling flow seems less intense than that measured experimentally, this causes a locally lower interaction between the main swirling flow and the coolant coming from the first effusion holes, which therefore limits the mixing between the two streams. This fact could justify the lower predicted wall temperatures in the first part of the effusion plate.

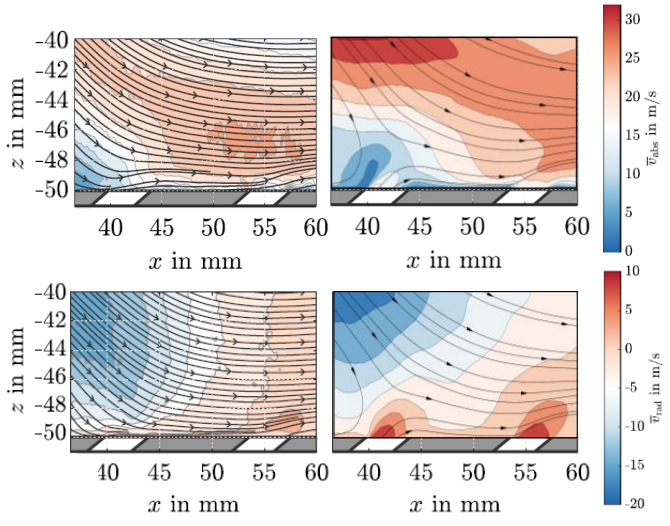

(A) (B)

FIGURE 18: VELOCITY DISTRIBUTION COMPARISON AT SECOND AND THIRD ROWS EXIT OF EFFUSION HOLES. EXPERIMENTAL RESULTS ADAPTED FROM [20] (A), U-THERM3D SIMULATION (B): VELOCITY MAGNITUDE (TOP) AND RADIAL VELOCITY (BOTTOM).

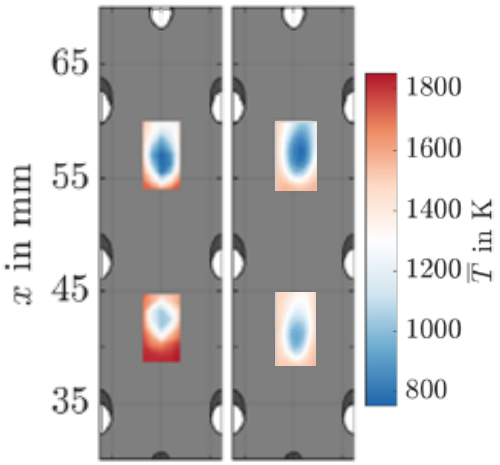

FIGURE 19: GAS PHASE TEMPERATURE DISTRIBUTION 0.5MM ABOVE THE COOLED LINER: (LEFT) EXPERIMENTAL MAPS ADAPTED FROM [20] AND (RIGHT) U-THERM3D SIMULATION

Focusing on the cooling system a possible cause could be the underprediction of the penetration of the jets exiting the effusion cooling holes, leading to a mass adduction regime that does not occur. The low mixing between coolant and main flows could generate a well-defined protective film that limits wall temperatures and at the same time, tends to raise the temperature of the gas phase before the zone of interaction between hot gas and coolant, as understandable from the first two graphs of Figure 13. To deeply understand the behavior of the cooling system, the gas phase temperature comparison at 0.5mm from the cooled wall is shown in Figure 19 to highlight the shape of the central effusion jets of the second and third rows (flow direction from bottom to top). Qualitatively, a good agreement with the experimental measurement is achieved. Comparing the bulk outlet velocity magnitude on the centerline of the second effusion row by estimating it with overall time-averaged quantities, the simulation predicts a different distribution of the coolant mass flow exiting the holes. In detail, the bulk velocity is 16 m/s, while for the numerical simulation it is 12.5 m/s. This data not only indicates that the simulation predicts a different wall coolant distribution from the experimental one but also confirms what was previously anticipated, i.e. that there is an overestimation of the heat removed from the cooling system.

5. CONCLUSION

In the present work, a numerical campaign was carried out for the first time on the TECFLAM gas turbine combustor model operating under close-to-reality conditions and with an effusion cooled liner. Several numerical approaches were compared, including a simplified version of the U-THERM3D multi-physics tool. In this preliminary approach, it was decided to neglect the radiative heat transfer due to the assumption of the low emissivity of methane flames, whereas a uniform temperature was imposed to simplify the modeling of the quartz walls.

The results obtained were compared with available experimental data, both in terms of aerothermal fields and solid wall temperatures. SBES approaches have been shown to predict the velocity, turbulence, and temperature fields accurately compared to the steady approach, except for the area where the fuel pilot jet develops. As shown, the behavior of the pilot jet was highly dependent on the conditions imposed on the quartz walls as they have a non-negligible impact on flame heat loss and consequently on the flow field within the combustion chamber. However, the proven effectiveness of the loosely coupled strategy is highlighted since it allows to properly take into account the heat losses related to the solid heat transfer. Therefore, it is evident how it is mandatory employing a multi-physics approach for a reliable prediction of the combustor aerothermal fields is since an adiabatic simulation leads inevitably to an overestimation of the temperatures.

The wall temperature map obtained from the simplified version of the U-THERM3D approach correctly predicts the experimental pattern, although an underprediction of approximately 100K is computed. The overestimation of the heat removed by the effusion system is mainly due to the weak interaction between the main and the coolant flows, which instead uniformly protects the liner. For an improvement in this sense, it is probably necessary to include the modeling of radiation and the related emissive behavior of the quartz since the test case proved to be extremely sensitive to these factors. However, a significant improvement with respect to a RANS calculation is obtained thanks to the resolution of the largest scales of the turbulence spectrum with an affordable computational cost. Moreover, a more accurate prediction of the reactive flow field thanks to a scale resolving approach permits an improvement of the prediction of flame-wall interaction and so of the wall heat fluxes and temperatures.

ACKNOWLEDGEMENTS

The authors would like to thank Professor A. Dreizler from Technischen Universität Darmstadt for providing clarification of the experimental test and the documentation needed to derive the boundary conditions for the numerical simulations. The results shown were obtained within the European project ACROSS (HPC Big DAta ArtifiCial intelligence cross Stack PlatfoRm TOwardS ExaScale). This project has received funding from the European High-Performance Computing Joint Undertaking (JU) under grant agreement No 955648. The JU receives support from the European Union's Horizon 2020 research and innovation programme and Italy, France, Czech Republic, United Kingdom, Greece, Netherlands, Germany, Norway. Therefore, the authors wish also to gratefully acknowledge ACROSS Consortium for the kind permission of publishing the results herein

REFERENCES

[1] K. M. B. Gustafsson and T. G. Johansson, "An Experimental Study of Surface Temperature Distribution on Effusion-Cooled Plates," *Journal of Engineering for Gas Turbines and Power*, vol. 123, no. 2, pp. 308–316, Apr. 2001, doi: 10.1115/1.1364496.

[2] G. E. Andrews, A. A. Asere, M. L. Gupta, and M. C. Mkpadi, “Full Coverage Discrete Hole Film Cooling: The Influence of Hole Size,” Mar. 1985. doi: 10.1115/85-GT-47.

[3] J. L. Florenciano and P. Bruel, “LES fluid–solid coupled calculations for the assessment of heat transfer coefficient correlations over multi-perforated walls,” *Aerospace Science and Technology*, vol. 53, pp. 61–73, Jun. 2016, doi: 10.1016/j.ast.2016.03.004.

[4] M. Darecki *et al.*, “Flightpath 2050: Europe’s Vision for Aviation: Report of the High Level Group,” *Publications Office of the European Union: Luxembourg*, 2011.

[5] R. M. Arnaldo Valdés, S. Burmaoglu, V. Tucci, L. M. Braga da Costa Campos, L. Mattera, and V. F. Gomez Comendador, “Flight Path 2050 and ACARE Goals for Maintaining and Extending Industrial Leadership in Aviation: A Map of the Aviation Technology Space.,” *Sustainability*, vol. 11, no. 7, p. 2065, Apr. 2019, doi: 10.3390/su11072065.

[6] J. J. McGuirk, “The aerodynamic challenges of aeroengine gas-turbine combustion systems,” *The Aeronautical Journal*, vol. 118, no. 1204, pp. 557–599, Jun. 2014, doi: 10.1017/S0001924000009386.

[7] A. Andreini, R. Becchi, B. Facchini, L. Mazzei, A. Picchi, and F. Turrini, “Adiabatic Effectiveness and Flow Field Measurements in a Realistic Effusion Cooled Lean Burn Combustor,” *Journal of Engineering for Gas Turbines and Power*, vol. 138, no. 3, Mar. 2016, doi: 10.1115/1.4031309/473643.

[8] A. Andreini, R. Becchi, B. Facchini, A. Picchi, and A. Peschiulli, “The effect of effusion holes inclination angle on the adiabatic film cooling effectiveness in a three-sector gas turbine combustor rig with a realistic swirling flow,” *International Journal of Thermal Sciences*, vol. 121, pp. 75–88, Nov. 2017, doi: 10.1016/J.IJTHERMALSCI.2017.07.003.

[9] B. Wurm, A. Schulz, H.-J. Bauer, and M. Gerendas, “Impact of Swirl Flow on the Cooling Performance of an Effusion Cooled Combustor Liner,” *Journal of Engineering for Gas Turbines and Power*, vol. 134, no. 12, Dec. 2012, doi: 10.1115/1.4007332.

[10] B. Wurm, A. Schulz, H.-J. Bauer, and M. Gerendas, “Impact of Swirl Flow on the Penetration Behaviour and Cooling Performance of a Starter Cooling Film in Modern Lean Operating Combustion Chambers,” Jun. 2014. doi: 10.1115/GT2014-25520.

[11] P. R. Spalart, “Detached-Eddy Simulation,” *Annual Review of Fluid Mechanics*, vol. 41, no. 1, pp. 181–202, Jan. 2009, doi: 10.1146/annurev.fluid.010908.165130.

[12] S. Puggelli, D. Bertini, L. Mazzei, and A. Andreini, “Assessment of Scale-Resolved Computational Fluid Dynamics Methods for the Investigation of Lean Burn Spray Flames,” *Journal of Engineering for Gas Turbines and Power*, vol. 139, no. 2, Feb. 2017, doi: 10.1115/1.4034194/374418.

[13] P. R. Spalart, S. Deck, M. L. Shur, K. D. Squires, M. Kh. Strelets, and A. Travin, “A New Version of Detached-eddy Simulation, Resistant to Ambiguous Grid Densities,” *Theoretical and Computational Fluid Dynamics*, vol. 20, no. 3, pp. 181–195, Jul. 2006, doi: 10.1007/s00162-006-0015-0.

[14] D. Bertini *et al.*, “Numerical and Experimental Investigation on an Effusion-Cooled Lean Burn Aeronautical Combustor: Aerothermal Field and Metal Temperature,” Jun. 2018. doi: 10.1115/GT2018-76779.

[15] L. He and M. Fadl, “Multi-scale time integration for transient conjugate heat transfer,” *International Journal for Numerical Methods in Fluids*, vol. 83, no. 12, pp. 887–904, Apr. 2017, doi: 10.1002/FLD.4295.

[16] D. Bertini, L. Mazzei, A. Andreini, and B. Facchini, “Multiphysics Numerical Investigation of an Aeronautical Lean Burn Combustor,” Jun. 2019. doi: 10.1115/GT2019-91437.

[17] S. Paccati, D. Bertini, L. Mazzei, S. Puggelli, and A. Andreini, “Large-Eddy Simulation of a Model Aero-Engine Sooting Flame With a Multiphysics Approach,” *Flow, Turbulence and Combustion*, vol. 106, no. 4, pp. 1329–1354, Apr. 2021, doi: 10.1007/s10494-020-00202-5.

[18] P. C. Nassini, D. Pampaloni, and A. Andreini, “Inclusion of flame stretch and heat loss in LES combustion model,” 2019, p. 020119. doi: 10.1063/1.5138852.

[19] J. Hermann, M. Greifenstein, B. Boehm, and A. Dreizler, “Experimental Investigation of Global Combustion Characteristics in an Effusion Cooled Single Sector Model Gas Turbine Combustor,” *Flow, Turbulence and Combustion*, vol. 102, no. 4, pp. 1025–1052, Apr. 2019, doi: 10.1007/s10494-018-9999-y.

[20] M. Greifenstein, J. Hermann, B. Boehm, and A. Dreizler, “Flame–cooling air interaction in an effusion-cooled model gas turbine combustor at elevated pressure,” *Experiments in Fluids*, vol. 60, no. 1, p. 10, Jan. 2019, doi: 10.1007/s00348-018-2656-3.

[21] ANSYS INC., “ANSYS Fluent Theory Guide, release 19.3.” 2019.

[22] F. Menter, “Stress-Blended Eddy Simulation (SBES)—A New Paradigm in Hybrid RANS-LES Modeling,” 2018, pp. 27–37. doi: 10.1007/978-3-319-70031-1_3.

[23] F. R. Menter, “Zonal two equation κ-ω turbulence models for aerodynamic flows,” *AIAA 23rd Fluid Dynamics, Plasmadynamics, and Lasers Conference, 1993*, 1993, doi: 10.2514/6.1993-2906.

[24] C. Meneveau and T. S. Lund, “The dynamic Smagorinsky model and scale-dependent coefficients in the viscous range of turbulence,” *Physics of Fluids*, vol. 9, no. 12, pp. 3932–3934, Dec. 1997, doi: 10.1063/1.869493.

[25] J. A. van Oijen, A. Donini, R. J. M. Bastiaans, J. H. M. ten Thije Boonkkamp, and L. P. H. de Goey, “State-of-the-art in premixed combustion modeling using flamelet generated manifolds,” *Progress in Energy and*

Combustion Science, vol. 57, pp. 30–74, Nov. 2016, doi: 10.1016/j.pecs.2016.07.001.

[26] A. Donini, R. J. M. Bastiaans, J. A. van Oijen, and L. P. H. de Goey, "The Implementation of Five-Dimensional FGM Combustion Model for the Simulation of a Gas Turbine Model Combustor," *Proceedings of the ASME Turbo Expo*, vol. 4A, Aug. 2015, doi: 10.1115/GT2015-42037.

[27] G. P. Smith *et al.*, "GRI-MECH 3.0 - http://www.me.berkeley.edu/gri_mech/."

[28] L. Mazzei, A. Andreini, B. Facchini, and L. Bellocci, "A 3D Coupled Approach for the Thermal Design of Aero-Engine Combustor Liners," *Proceedings of the ASME Turbo Expo*, vol. 5B-2016, Sep. 2016, doi: 10.1115/GT2016-56605.

[29] D. Bertini *et al.*, "Numerical and Experimental Investigation on an Effusion-Cooled Lean Burn Aeronautical Combustor: Aerothermal Field and Metal Temperature," *Proceedings of the ASME Turbo Expo*, vol. 5C-2018, Aug. 2018, doi: 10.1115/GT2018-76779.

[30] S. Paccati, D. Bertini, S. Puggelli, L. Mazzei, A. Andreini, and B. Facchini, "Numerical analyses of a high pressure sooting flame with multiphysics approach," *Energy Procedia*, vol. 148, pp. 591–598, Aug. 2018, doi: 10.1016/j.egypro.2018.08.146.

[31] A. Andreini, R. da Soghe, B. Facchini, L. Mazzei, S. Colantuoni, and F. Turrini, "Local source based CFD modeling of effusion cooling holes: Validation and application to an actual combustor test case," *Journal of Engineering for Gas Turbines and Power*, vol. 136, no. 1, Jan. 2014, doi: 10.1115/1.4025316/373743.

[32] H. Chanson, *Applied hydrodynamics: an introduction to ideal and real fluid flows*. CRC press, 2009.

[33] D. G. Goodwin, R. L. Speth, H. K. Moffat, and B. W. Weber, "Cantera: An Object-oriented Software Toolkit for Chemical Kinetics, Thermodynamics, and Transport Processes," *2021*.

[34] I. B. Celik, Z. N. Cehreli, and I. Yavuz, "Index of Resolution Quality for Large Eddy Simulations," *Journal of Fluids Engineering*, vol. 127, no. 5, pp. 949–958, Sep. 2005, doi: 10.1115/1.1990201.

[35] S. B. Pope, "Ten questions concerning the large-eddy simulation of turbulent flows," *New Journal of Physics*, vol. 6, pp. 35–35, Mar. 2004, doi: 10.1088/1367-2630/6/1/035.

[36] G. Boudier, L. Y. M. Gicquel, and T. J. Poinsot, "Effects of mesh resolution on large eddy simulation of reacting flows in complex geometry combustors," *Combustion and Flame*, vol. 155, no. 1–2, pp. 196–214, Oct. 2008, doi: 10.1016/j.combustflame.2008.04.013.

[37] P. C. Nassini, D. Pampaloni, R. Meloni, and A. Andreini, "Lean blow-out prediction in an industrial gas turbine combustor through a LES-based CFD analysis," *Combustion and Flame*, vol. 229, p. 111391, Jul. 2021, doi: 10.1016/j.combustflame.2021.02.037.